Published in final edited form as:
Neuroimage. 2014 August 1; 96: 88–94. doi:10.1016/j.neuroimage.2014.03.065.

Graph Theoretical Analysis of Resting-State MEG data: Identifying Interhemispheric Connectivity and the Default Mode

Joseph A. Maldjian[1,2,3], **Elizabeth M. Davenport**[1,3,4], and **Christopher T. Whitlow**[1,2,5]

[1]Advanced Neuroscience Imaging Research (ANSIR) Laboratory, Wake Forest School of Medicine, Winston-Salem, NC 27157-1088, USA

[2]Department of Radiology, Wake Forest School of Medicine, Winston-Salem, NC 27157-1088, USA

[3]Department of Biomedical Engineering, Wake Forest School of Medicine, Winston-Salem, NC 27157-1088, USA

[4]Virginia Tech – Wake Forest School of Biomedical Engineering, Wake Forest School of Medicine, Winston-Salem, NC 27157-1088, USA

[5]Translational Science Institute, Wake Forest School of Medicine, Winston-Salem, NC 27157-1088, USA

Abstract

Interhemispheric connectivity with resting state MEG has been elusive, and demonstration of the default mode network (DMN) yet more challenging. Recent seed-based MEG analyses have shown interhemispheric connectivity using power envelope correlations. The purpose of this study is to compare graph theoretic maps of brain connectivity generated using MEG with and without signal leakage correction to evaluate for the presence of interhemispheric connectivity.

Eight minutes of resting state eyes-open MEG data were obtained in 22 normal male subjects enrolled in an IRB-approved study (ages 16–18). Data were processed using an in-house automated MEG processing pipeline and projected into standard (MNI) source space at 7 mm resolution using a scalar beamformer. Mean beta-band amplitude was sampled at 2.5 second epochs from the source space time series. Leakage correction was performed in the time domain of the source space beam-formed signal prior to amplitude transformation. Graph theoretic voxel-wise source space correlation connectivity analysis was performed for leakage-corrected and uncorrected data. Degree maps were thresholded across subjects for the top 20% of connected nodes to identify hubs. Additional degree maps for sensory, visual, motor, and temporal regions were generated to identify interhemispheric connectivity using laterality indices. Hubs for the uncorrected MEG networks were predominantly symmetric and midline, bearing some

Correspondence to: **Joseph Maldjian, M.D.**, Department of Radiology, Wake Forest University Health Sciences, Winston-Salem, NC, USA 27157, maldjian@wakehealth.edu.

resemblance to fMRI networks. These included the cingulate cortex, bilateral inferior frontal lobes, bilateral hippocampal formations and bilateral cerebellar hemispheres. These uncorrected networks however, demonstrated little to no interhemispheric connectivity using the ROI-based degree maps. Leakage corrected MEG data identified the DMN, with hubs in the posterior cingulate and biparietal areas. These corrected networks demonstrated robust interhemispheric connectivity for the ROI-based degree maps. Graph theoretic analysis of MEG resting state data without signal leakage correction can demonstrate symmetric networks with some resemblance to fMRI networks. These networks however, are an artifact of high local correlation from signal leakage and lack interhemispheric connectivity. Following signal leakage correction, MEG hubs emerge in the DMN, with strong interhemispheric connectivity.

Keywords

magnetoencephalography; graph theory; default mode network; interhemispheric connectivity; fMRI = functional MRI; PC = phase coherence; PLI = phase lag index (PLI); icoh = imaginary coherence

1. Introduction

MEG is a non-invasive imaging method that detects the magnetic fields induced by neuronal electrical activity, with millisecond time scale resolution (Schwartz et al., 2010). Although MEG has a spatial resolution that is coarse compared to conventional structural MRI, the comparison becomes more favorable compared to the typical fMRI resolutions in the range of 3 – 4 mm. The high temporal resolution and favorable spatial resolution makes MEG a very attractive modality for studies of brain connectivity.

Graph theoretic analysis of resting state imaging data represents a powerful method for demonstrating relationships in brain connectivity. Hallmarks of resting state fMRI studies are the presence of robust interhemispheric connectivity and identification of the default mode network (DMN). Despite this robust connectivity for fMRI studies, identifying interhemispheric connectivity using MEG resting state data has been more elusive. Identification of the DMN with MEG has been even more obscure. Some recent MEG studies however, have noted connections between regions within the DMN (Brookes et al., 2011b; de Pasquale et al., 2010).

MEG methods for characterizing whole brain functional network connectivity may be particularly well suited to investigate diseases that affect endothelial function and CBF, such as diabetes and neurodegenerative disorders. In such diseases, there may be a degree of uncoupling between CBF/metabolism and neural activity that limits the ability of BOLD fMRI network methods to accurately reflect hemodynamic responses of disease-associated neuronal network dysfunction. Compared to the fMRI literature, however, there has been a relative paucity of graph theoretic analyses of MEG data. Much of the MEG literature has been focused on taskbased studies. For MEG analyses, the presence of a baseline condition considerably simplifies the analysis by offering a direct method of center volume conduction artifact suppression through subtraction. Despite the extensive interest in resting state connectivity initiated by fMRI studies, only recently has there been some attention directed

to resting-state analyses of MEG data as well as to the additional processing requirements. Many of these recent MEG-based studies have focused on sensor-space connectivity measures, which are problematic in several regards. The sensor-spaced measurements are known to suffer from signal leakage, resulting in artificially elevated measures of connectivity between sensors. Additionally, the spatial maps obtained from these sensor-space analyses do not convey the actual regional brain activity, and have no resemblance to brain-space fMRI connectivity. Source-space analyses of MEG data can be performed using beam-forming techniques (Huang et al., 2004; Robinson, 2004). These techniques have been applied to resting state MEG data using a variety of connectivity metrics. While it is tempting to use source space MEG time series directly for network analyses, unlike for fMRI, direct correlation analyses of the MEG beamformer reconstructed source time-courses are problematic, and can show correlations from spurious, field spread, and volume conduction interactions, manifesting as locking with zero-phase lags. A variety of connectivity metrics have been developed to circumvent these problems. For example, the phase coherence (PC), the phase lag index (PLI), and imaginary coherence (icoh) of the MEG time courses have been used as connectivity measures (Hillebrand et al., 2012; Ortiz et al., 2012; Stam et al., 2009; Stam et al., 2007; Tewarie et al., 2013; Vinck et al., 2011). There have been several studies using these metrics to identify MEG source space networks. An interesting aspect of these measures is that they do not typically demonstrate interhemispheric connectivity, which is in striking contrast to the fMRI-based networks that routinely demonstrate homologous interhemispheric connections. This makes comparison to fMRI difficult, and complicates interpretation of these MEG networks. Only recently has Pearson correlation, using the power-envelope transformation (e.g. Hilbert transform) of the voxel time-courses, demonstrated the ability to identify interhemispheric MEG correlations (Brookes et al., 2011a; Brookes et al., 2011b). Resting state MEG connectivity maps generated using the Hilbert transform resemble fMRI resting networks closely (Brookes et al., 2011a; Brookes et al., 2011b), whereas connectivity maps generated using PC, PLI, and icoh appear to have limited similarity to fMRI and to each other (Hillebrand et al., 2012; Stam et al., 2007).

Many of the common MEG connectivity metrics (PC, PLI, icoh) are used to circumvent the problem of signal leakage. These approaches typically extract the non-0 phase lag connectivity between signals. Spurious correlation can result from “leakage” of signal from a reference site to nearby locations such that the source signal is sensitive to the same true sources as the reference signal (Hipp et al., 2012). Approaches based on regression in the frequency or time-domain have been proposed as alternative means to correct for signal leakage for seedbased connectivity analyses (Brookes et al., 2012; Hall et al., 2013; Hipp et al., 2012; Woolrich et al., 2013).

The purpose of this study is to compare graph theoretic maps of brain connectivity generated using MEG with and without signal leakage correction and evaluate for the presence of interhemispheric connectivity. We use beam-former source space analyses, and a novel meanamplitude based connectivity metric with voxel-wise whole-brain graph theoretic analysis to identify the regions of highest connectivity and map connectivity to a variety of primary sensorymotor areas. This study demonstrates that MEG graph theory studies must

account for spatial leakage, especially with reference to the DMN, otherwise, the networks identified are likely artifactual and reflect high local correlation from spatial leakage.

2. METHODS

Eight minutes of resting state eyes-open MEG data were obtained in 22 normal male subjects (ages 16–18) enrolled in an IRB-approved study (Cobb et al., 2013; Urban et al., 2013). Data were processed using an in-house automated MEG processing pipeline and projected into standard (MNI) source space at 7 mm resolution using a scalar beamformer (Robinson, 2004). Mean beta-band amplitude was sampled at 2.5 second epochs from the 4D source space time series. Leakage correction was performed in the time domain of the source space beam-formed signal prior to amplitude transformation. Graph theoretic voxel-wise source space correlation connectivity analysis was performed for corrected and uncorrected data. Degree maps were thresholded across subjects for the top 20% of connected nodes to identify hubs. Additional degree maps for motor, sensory, visual, and temporal regions were generated to identify interhemispheric connectivity using laterality indices. Additional details of the methods are provided in the appendix.

3. Results

3.1 Scale-free behavior

All subjects demonstrated similar scale free behavior for both corrected and uncorrected networks. The degree distribution for the MEG networks followed an exponentially truncated power law, as has been demonstrated for many other biologic networks (Achard et al., 2006; Bassett et al., 2006; Gong et al., 2009; He et al., 2007; Iturria-Medina et al., 2008).

3.2 Network Hubs

Figure 1A demonstrates the hub heat map for the non-corrected MEG network for the top 20% of connections across subjects. Hubs identified include the posterior and mid cingulate cortex, bilateral inferior frontal lobes, bilateral hippocampal formations and bilateral cerebellar hemispheres. Hubs in the uncorrected data were highly symmetric with some resemblance to fMRI maps of the DMN in the posterior cingulate. Figure 1B demonstrates the hub heat map for the leakage corrected MEG networks across subjects. Hubs identified included the posterior cingulate and bilateral parietal areas.

The laterality indices for the ROI-based connections are listed in Table 1. For the uncorrected data, the mean laterality indices for the pre_l was 0.92, pre_r was −0.92, post_l was 0.86, post_r was −0.90, calc_l was 0.08, calc_r was −0.55, temp_l was 0.98, and temp_r was − 0.98. The leakage-corrected mean laterality indices for the pre_l was 0.58, pre_r was −0.52, post_l was 0.44, post_r was −0.51, calc_l was −0.12, calc_r was −0.34, temp_l was 0.53, and temp_r was −0.58. Twenty three of the possible 176 ROIs (8 ROIs×22 subjects) for the uncorrected data demonstrated no interhemispheric connections, compared with 8/176 for the corrected data. One hundred and two of the possible 176 ROIs for the uncorrected data had very sparse interhemispheric connections (LI > 0.9), in comparison to only 18/176 for the corrected data. The calcarine ROIs were the only areas that demonstrated any significant contralateral connectivity for the uncorrected data. Visual

inspection of the calcarine maps from the uncorrected data demonstrated the vast majority of the contralateral connections to be just barely crossing the mid-line, representing leakage from the large midline portion of the primary ROI (figure 3A). For the more lateralized primary ROI (e.g., left and right middle temporal gyrus), only 1 subject for the uncorrected data demonstrated any significant contralateral connectivity (e.g. LI < < 0.9) with the majority of laterality indices in the 0.99 – 1.0 range. A similar analysis was also done for the hippocampus hub identified from the uncorrected data. This demonstrated very few contralateral connections for either hippocampus (mean LI > 0.95) with the majority of subjects having laterality indices of 0.99 − 1.

Figure 2A is a group connectivity map of voxels connected to the right motor cortex (pre_r) for the non-corrected MEG data. The area in gold represents the seed. All connections are local to the seed with no interhemispheric connectivity identified. Following signal leakage correction, robust contralateral motor cortex connectivity emerges. Similarly, the group connectivity map for the right post-central gyrus seed demonstrates little to no contralateral connectivity for the uncorrected data (figure 3A). Following signal leakage correction, robust connectivity to the contralateral post-central gyrus emerges, in addition to connectivity to other motor sub-systems including the supplementary motor area bilaterally at the midline (Figure 3B). A similar pattern of robust contralateral connectivity following leakage correction is identified for the calcarine cortex (figure 4) and the middle temporal gyrus (figure 5). In addition to connectivity to the contralateral seed area, the leakage corrected networks demonstrate connections to other distributed subsystems. For the uncorrected data, the right temporal lobe seed demonstrates almost exclusively unilateral connections (figure 5 A). For the corrected data however, the right temporal lobe seed demonstrates connectivity to the left temporal lobe as well as distributed areas in the frontal lobes and basal ganglia bilaterally (figure 5B). The histogram plot of correlation values for the uncorrected data (Figure 6, left) demonstrates a large number of high-correlation edges. The mean of the correlation cutoffs required to satisfy the threshold criterion was 0.56 (sd=0.08). The corrected data (Figure 6, middle) demonstrates markedly fewer high correlation edges, with a corresponding mean correlation cutoff =0.41 (sd=0.12) for the same threshold. This is also reflected in the difference histogram plot, demonstrating a shift towards high correlation edges for the uncorrected data (Figure 6, right).

Sensitivity analyses at costs from 0.01 – 0.3 demonstrated similar hub topology across this range. Interhemispheric connectivity for the uncorrected ROI-based networks decreased further at the lower costs, and increased for the higher costs (see Supplementary Tables). As the cost threshold increases, the correlation threshold relaxes allowing more connections to survive the threshold criterion. At the higher costs (> 0.1), there was also a lack of specificity in the interhemispheric connections with connectivity present to almost all voxels in the brain.

4. Discussion

The demonstration of interhemispheric connectivity with resting state MEG has been elusive. Only recently have methods using power envelope transformations been shown to generate connectivity maps with similarity to fMRI. These have been demonstrated using

both ICA and seed correlation based methods (Brookes et al., 2011a; Brookes et al., 2011b; Brookes et al., 2012; Luckhoo et al., 2012). In this study, we introduce a mean amplitude analysis method for graph theoretic analyses. The initial analyses with this technique generate connectivity degree maps that bear some resemblance to fMRI connectivity. Areas of high degree were identified in the posterior cingulate cortex, an area represented in the default mode. Additional midline areas were also revealed, including the bifrontal regions and the hippocampal structures. While it is tempting to assign significance to these areas in terms of the similarity to fMRI and inherent symmetry, closer inspection of the connectivity reveals these areas of high degree to be completely artifactual, related to spatial leakage of the MEG signal. None of these areas of high degree demonstrate any significant interhemispheric connectivity. The connections are all driven locally by surrounding areas of high correlation. This is further demonstrated by the higher correlation threshold required to satisfy the edge density criterion.

4.1 Signal Leakage Correction

The signal leakage correction applied here markedly reduces local correlations and allows the interhemispheric correlations to appear. Although these correlations are also present in the non-corrected data, the high local correlations dominate the connectivity and drive the correlation thresholds so high that the interhemispheric connections do not survive. Following signal leakage correction the pattern of highly connected hubs closely resembles the default mode network (DMN) identified in fMRI studies, involving the posterior cingulate and biparietal areas. This is an important finding, as most previous resting-state MEG connectivity studies have failed to effectively identify the DMN. It is also interesting that we were able to identify the DMN in the beta band. Our choice of beta-band was based on previous ICA-based work demonstrating the most similarity of MEG to fMRI networks in the beta-band (Brookes et al., 2011b). In this same paper, however, DMN-like topology was only identified for the alpha band (biparietal activity, but without posterior cingulate). In a study by Pasquale et al looking at the DMN using a maximum correlation window approach, the most fMRI-like topology for the DMN was found in theta and alpha bands (de Pasquale et al., 2010). In a study of MEG and acupuncture, the highest correlation between DMN structures was found for the alpha band (You et al., 2013). Our analyses were limited to a single band due to the computational burden of the leakage correction, which required approximately 24 hours of processing time per subject. Investigation of leakage-corrected network topology in other bands may provide additional insights into DMN activity.

The degree distribution for both the corrected and uncorrected MEG networks followed a scale-free distribution, most closely approximated by a truncated exponential power law. Similar behavior has been observed for fMRI networks, as well as a wide-variety of biological networks. This behavior implies that highly connected nodes tend to accrue more connections, however, this falls off at the extreme end of the distribution.

Signal leakage correction was done in the time domain as a 0-lag regression between each voxel and all other voxels. A similar correction can be performed in the frequency domain. When performed in the time domain, the correction would need to be performed separately for each frequency band of interest, whereas in the frequency domain, the correction can be

performed once for all frequency bands (Brookes et al., 2012). For seed-based analyses, the computational demand of the signal leakage correction is relatively minimal. However, for a graph theoretic analysis in which correlations are computed between all voxel time courses (essentially an all-to-all seed based analysis), the computational and memory requirements become demanding. This required incorporating the regression into the graph theoretic analysis pipeline as a voxel-wise iterative procedure immediately following the beamformer source space projection. In our standard MEG processing pipeline without leakage correction, computation time from sensor space through beamformer source space projection, power envelope transformation and downsampling to 1 Hz takes approximately 10 minutes, with the final Cij computation accomplished within 1 hour on a 12-node system with 192 GB of RAM. In comparison, the signal leakage correction for 1 subject from sensor space through final Cij computation requires approximately 1 day of processing time using the same system. The leakage correction is performed immediately following beamformer source projection sampled at 100 Hz to avoid loss of information in the 0-lag signal coherence that would occur following any power envelope or downsampling steps. Additionally, the memory requirements make it prohibitive to generate a group connectivity analysis with leakage correction by simply concatenating voxel time courses on current systems.

4.2 Interhemispheric Connectivity

Previous studies have performed graph theoretic analyses using other connectivity metrics (e.g., phase lag coherence, coherence, imaginary coherence). The phase-lag index has been demonstrated to have less sensitivity to spurious correlations from common sources as compared to phase coherence and imaginary coherence (Stam et al., 2007), and has been used in several graph theoretic studies of source space connectivity (Hillebrand et al., 2012; Van Dellen et al., 2013). In these studies, however, connectivity computations were reduced to a single representative voxel from each region of interest (ROI). The use of pre-defined ROIs guarantees a result, circumventing the issue altogether. Graph theoretic MEG studies of the DMN have also typically used predefined ROIs to compare connectivity (Franzen et al., 2013; Van Dellen et al., 2013; Wilson et al., 2013; You et al., 2013), rather than using direct data-driven extraction of the network. Recent work looking at DMN connectivity has suggested that non-stationarity in the MEG signal may be the cause of the lack of interhemispheric connectivity in MEG resting state studies. De Pasquale et al introduced a maximal correlation window approach to essentially search for the signal time-lag that provides an optimal correlation for identifying interhemispheric network correlations, especially with regard to the DMN (de Pasquale et al., 2010). Interestingly, the power envelope based transforms have demonstrated interhemispheric connectivity without the need for lagging correlation signal time courses. Similarly, here we demonstrate robust interhemispheric network correlations with mean beta amplitude using graph theoretic analyses and signal leakage correction. Without leakage corrections, the MEG graph theoretic maps have little to no interhemispheric connectivity. Following leakage correction, interhemispheric connectivity is observed for the primary sensory modalities including motor and visual cortex, as well as temporal lobe cortical regions.

4.3 Limitations

Limitations of this work include the relatively small sample size and unique characteristics of the subject population. An important caveat is that our sample was limited to adolescent males, as this was drawn from a larger study of sports-related impacts in high school football players. The brain networks in this population may not be directly comparable to the adult networks generated using fMRI. Additionally, our analyses were limited to beta band filtered data. The appearance of networks for other frequency bands is likely to be quite different. Also, these networks were generated based on a 2.5 second sampling period using mean beta amplitude. Networks generated at higher sampling frequencies and other signal transformation strategies may demonstrate additional properties. This method of leakage correction only corrects for leakage from one seed voxel for each correlation computation. This may result in a correlation pattern surrounding the target voxel that is spatially inhomogeneous (Brookes et al., 2012). In addition, the technique will remove any “true” neuronal signal with a zero phase lag. Graph theoretic networks can be generated using a variety of edge criteria and thresholds, and may reveal additional hubs, especially as the threshold criterion is relaxed. In order to investigate threshold related effects, we repeated the analyses using a range of costs (0.01, 0.05, 0.1, 0.2, and 0.3) with similar results in hub topology. The presence of interhemispheric connectivity however, was affected by the threshold. As the correlation threshold is relaxed (at higher cost ranges), interhemispheric connectivity increases at the expense of specificity in the contralateral connected regions.

5. Conclusion

Graph theoretic analysis of MEG resting state data without signal leakage correction can demonstrate symmetric networks with some resemblance to fMRI networks. These networks however, are an artifact of high local correlation from signal leakage and lack interhemispheric connectivity. Following signal leakage correction, MEG hubs emerge in the DMN, with strong interhemispheric connectivity. We additionally present a novel mean-amplitude based metric for conducting MEG resting state studies that demonstrates robust interhemispheric connectivity.

Supplementary Material

Refer to Web version on PubMed Central for supplementary material.

Acknowledgments

The authors would like to thank the Reagan High School, especially Ashley Lake, ATC (Reagan High School), Corbin Ratcliffe, Lauren Smith and the football program. Thank you to Ben Wagner for computer programming support. Technical support for MEG data acquisition was provided by Ina McGowin, Justin Rowley, Greg Alberto, Taylor Bungo, Cassie Cornell and Dr. Dwayne Godwin through the Department of Neurology MEG Center. Technical support for MRI data acquisition was provided by Sandra Kaminsky and Debra Fuller through the Center for Biomolecular Imaging.

Special thanks to the Childress Institute for Pediatric Trauma at Wake Forest Baptist Medical Center for providing support to us and our collaborators, Joel Stitzel and Alex Powers, on the pediatric football study. This material is based upon work supported by the National Science Foundation Graduate Research Fellowship under Grant No. DGE-0907738 to EMD. Any opinion, findings, and conclusions or recommendations expressed in this material are those of the authors(s) and do not necessarily reflect the views of the National Science Foundation. Support for this research was also provided by NIH grants NS058700 (PI: Don Bowden) and NS0075107 (JAM).

References

Achard S, Salvador R, Whitcher B, Suckling J, Bullmore E. A resilient, low-frequency, small-world human brain functional network with highly connected association cortical hubs. J Neurosci. 2006; 26:63–72. [PubMed: 16399673]

Bassett DS, Meyer-Lindenberg A, Achard S, Duke T, Bullmore E. Adaptive reconfiguration of fractal small-world human brain functional networks. Proc Natl Acad Sci U S A. 2006; 103:19518–19523. [PubMed: 17159150]

Brookes MJ, Hale JR, Zumer JM, Stevenson CM, Francis ST, Barnes GR, Owen JP, Morris PG, Nagarajan SS. Measuring functional connectivity using MEG: methodology and comparison with fcMRI. Neuroimage. 2011a; 56:1082–1104. [PubMed: 21352925]

Brookes MJ, Woolrich M, Luckhoo H, Price D, Hale JR, Stephenson MC, Barnes GR, Smith SM, Morris PG. Investigating the electrophysiological basis of resting state networks using magnetoencephalography. Proceedings of the National Academy of Sciences of the United States of America. 2011b; 108:16783–16788. [PubMed: 21930901]

Brookes MJ, Woolrich MW, Barnes GR. Measuring functional connectivity in MEG: a multivariate approach insensitive to linear source leakage. Neuroimage. 2012; 63:910–920. [PubMed: 22484306]

Cobb BR, Urban JE, Davenport EM, Rowson S, Duma SM, Maldjian JA, Whitlow CT, Powers AK, Stitzel JD. Head Impact Exposure in Youth Football: Elementary School Ages 9–12 Years and the Effect of Practice Structure. Ann Biomed Eng. 2013

de Pasquale F, Della Penna S, Snyder AZ, Lewis C, Mantini D, Marzetti L, Belardinelli P, Ciancetta L, Pizzella V, Romani GL, Corbetta M. Temporal dynamics of spontaneous MEG activity in brain networks. Proceedings of the National Academy of Sciences of the United States of America. 2010; 107:6040–6045. [PubMed: 20304792]

Franzen JD, Heinrichs-Graham E, White ML, Wetzel MW, Knott NL, Wilson TW. Atypical coupling between posterior regions of the default mode network in attention-deficit/hyperactivity disorder: a pharmaco-magnetoencephalography study. J Psychiatry Neurosci. 2013; 38:120054.

Gong G, He Y, Concha L, Lebel C, Gross DW, Evans AC, Beaulieu C. Mapping anatomical connectivity patterns of human cerebral cortex using in vivo diffusion tensor imaging tractography. Cereb Cortex. 2009; 19:524–536. [PubMed: 18567609]

Hall EL, Woolrich MW, Thomaz CE, Morris PG, Brookes MJ. Using variance information in magnetoencephalography measures of functional connectivity. Neuroimage. 2013; 67:203–212. [PubMed: 23165323]

He Y, Chen ZJ, Evans AC. Small-world anatomical networks in the human brain revealed by cortical thickness from MRI. Cereb Cortex. 2007; 17:2407–2419. [PubMed: 17204824]

Hillebrand A, Barnes GR, Bosboom JL, Berendse HW, Stam CJ. Frequency-dependent functional connectivity within resting-state networks: an atlas-based MEG beamformer solution. Neuroimage. 2012; 59:3909–3921. [PubMed: 22122866]

Hipp JF, Hawellek DJ, Corbetta M, Siegel M, Engel AK. Large-scale cortical correlation structure of spontaneous oscillatory activity. Nature neuroscience. 2012; 15:884–890.

Huang MX, Shih JJ, Lee RR, Harrington DL, Thoma RJ, Weisend MP, Hanlon F, Paulson KM, Li T, Martin K, Millers GA, Canive JM. Commonalities and differences among vectorized beamformers in electromagnetic source imaging. Brain Topogr. 2004; 16:139–158. [PubMed: 15162912]

Iturria-Medina Y, Sotero RC, Canales-Rodriguez EJ, Aleman-Gomez Y, Melie-Garcia L. Studying the human brain anatomical network via diffusion-weighted MRI and Graph Theory. Neuroimage. 2008; 40:1064–1076. [PubMed: 18272400]

Luckhoo H, Hale JR, Stokes MG, Nobre AC, Morris PG, Brookes MJ, Woolrich MW. Inferring task-related networks using independent component analysis in magnetoencephalography. Neuroimage. 2012; 62:530–541. [PubMed: 22569064]

Ortiz E, Stingl K, Münssinger J, Braun C, Preissl H, Belardinelli P. Weighted phase lag index and graph analysis: preliminary investigation of functional connectivity during resting state in children. Computational and mathematical methods in medicine 2012. 2012

Robinson SE. Localization of event-related activity by SAM(erf). Neurol Clin Neurophysiol. 2004; 2004:109. [PubMed: 16012649]

Schwartz ES, Edgar JC, Gaetz WC, Roberts TP. Magnetoencephalography. Pediatr Radiol. 2010; 40:50–58. [PubMed: 19937237]

Stam CJ, de Haan W, Daffertshofer A, Jones BF, Manshanden I, van Cappellen van Walsum AM, Montez T, Verbunt JPA, de Munck JC, van Dijk BW, Berendse HW, Scheltens P. Graph theoretical analysis of magnetoencephalographic functional connectivity in Alzheimer's disease. Brain: a journal of neurology. 2009; 132:213–224. [PubMed: 18952674]

Stam CJ, Nolte G, Daffertshofer A. Phase lag index: assessment of functional connectivity from multi channel EEG and MEG with diminished bias from common sources. Hum Brain Mapp. 2007; 28:1178–1193. [PubMed: 17266107]

Tewarie P, Hillebrand A, Schoonheim MM, van Dijk BW, Geurts JJG, Barkhof F, Polman CH, Stam CJ. Functional brain network analysis using minimum spanning trees in Multiple Sclerosis: An MEG source-space study. NeuroImage. 2013

Urban JE, Davenport EM, Golman AJ, Maldjian JA, Whitlow CT, Powers AK, Stitzel JD. Head Impact Exposure in Youth Football: High School Ages 14 to 18 Years and Cumulative Impact Analysis. Ann Biomed Eng. 2013

Van Dellen E, De Witt Hamer PC, Douw L, Klein M, Heimans JJ, Stam CJ, Hillebrand A. Connectivity in MEG resting-state networks increases after resective surgery for low-grade glioma and correlates with improved cognitive performance. NeuroImage: Clinical. 2013; 2:1–7. [PubMed: 24179752]

Vinck M, Oostenveld R, van Wingerden M, Battaglia F, Pennartz CMA. An improved index of phase-synchronization for electrophysiological data in the presence of volume-conduction, noise and sample-size bias. NeuroImage. 2011; 55:1548–1565. [PubMed: 21276857]

Wilson TW, Franzen JD, Heinrichs-Graham E, White ML, Knott NL, Wetzel MW. Broadband neurophysiological abnormalities in the medial prefrontal region of the default-mode network in adults with ADHD. Hum Brain Mapp. 2013; 34:566–574. [PubMed: 22102400]

Woolrich MW, Baker A, Luckhoo H, Mohseni H, Barnes G, Brookes M, Rezek L. Dynamic state allocation for MEG source reconstruction. Neuroimage. 2013

You Y, Bai L, Dai R, Cheng H, Liu Z, Wei W, Tian J. Altered hub configurations within default mode network following acupuncture at ST36: a multimodal investigation combining fMRI and MEG. PLoS One. 2013; 8:e64509. [PubMed: 23691237]

Highlights

- We compare graph theoretic MEG maps with and without leakage correction.
- We use a novel mean-amplitude metric for MEG connectivity analyses.
- Non-corrected graph theoretic MEG maps lack interhemispheric connectivity.
- Network hubs on graph theoretic MEG maps without leakage correction are artifacts.
- Interhemispheric connectivity and the DMN emerge on leakage-corrected MEG maps.

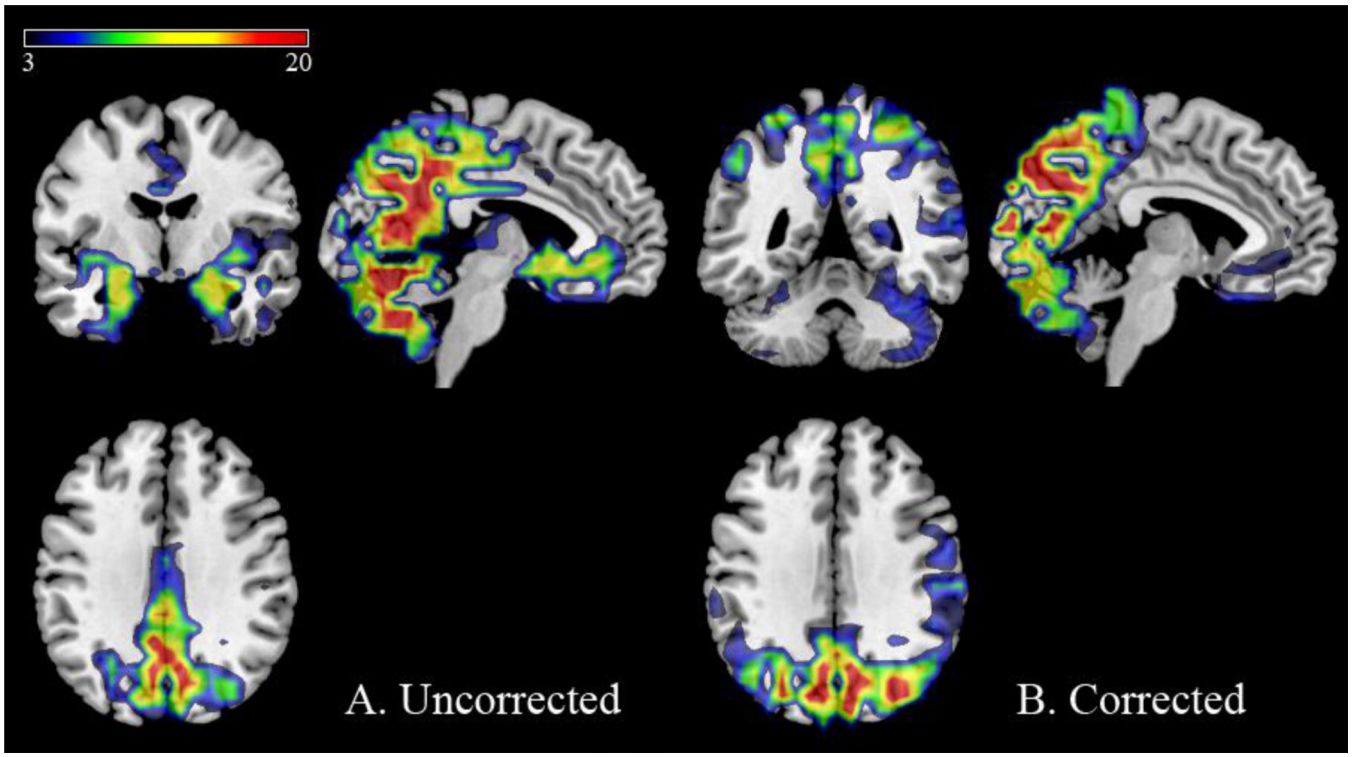

Figure 1.

Degree heat maps for the non-corrected (A) and corrected (B) MEG graph networks for the top 20% of connections across subjects (red is greatest overlap). Non-corrected network demonstrates hubs in the posterior and mid cingulate cortex, bilateral inferior frontal lobes, bilateral hippocampal formations and bilateral cerebellar hemispheres. Leakage corrected networks demonstrate hubs in the posterior cingulate and bilateral parietal lobes in areas known to be part of DMN from fMRI studies.

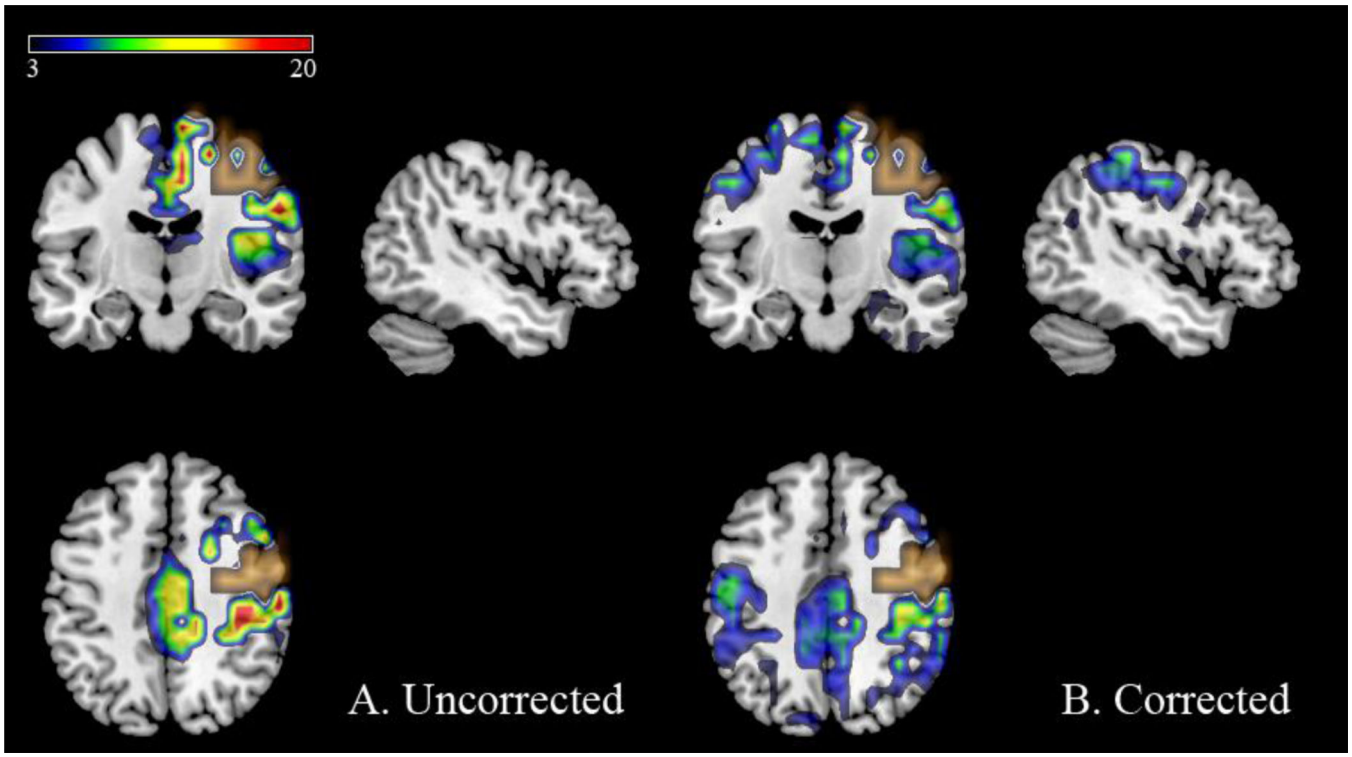

Figure 2.

Group connectivity heat map for voxels connected to the right motor cortex (pre_r) for the non-corrected MEG data (A) and corrected data (B). Maps were created by binarizing and summing ROI degree maps across subjects. The area in gold represents the seed ROI. Color represents the amount of connectivity overlap between subjects. Uncorrected data demonstrates no significant interhemispheric connections.

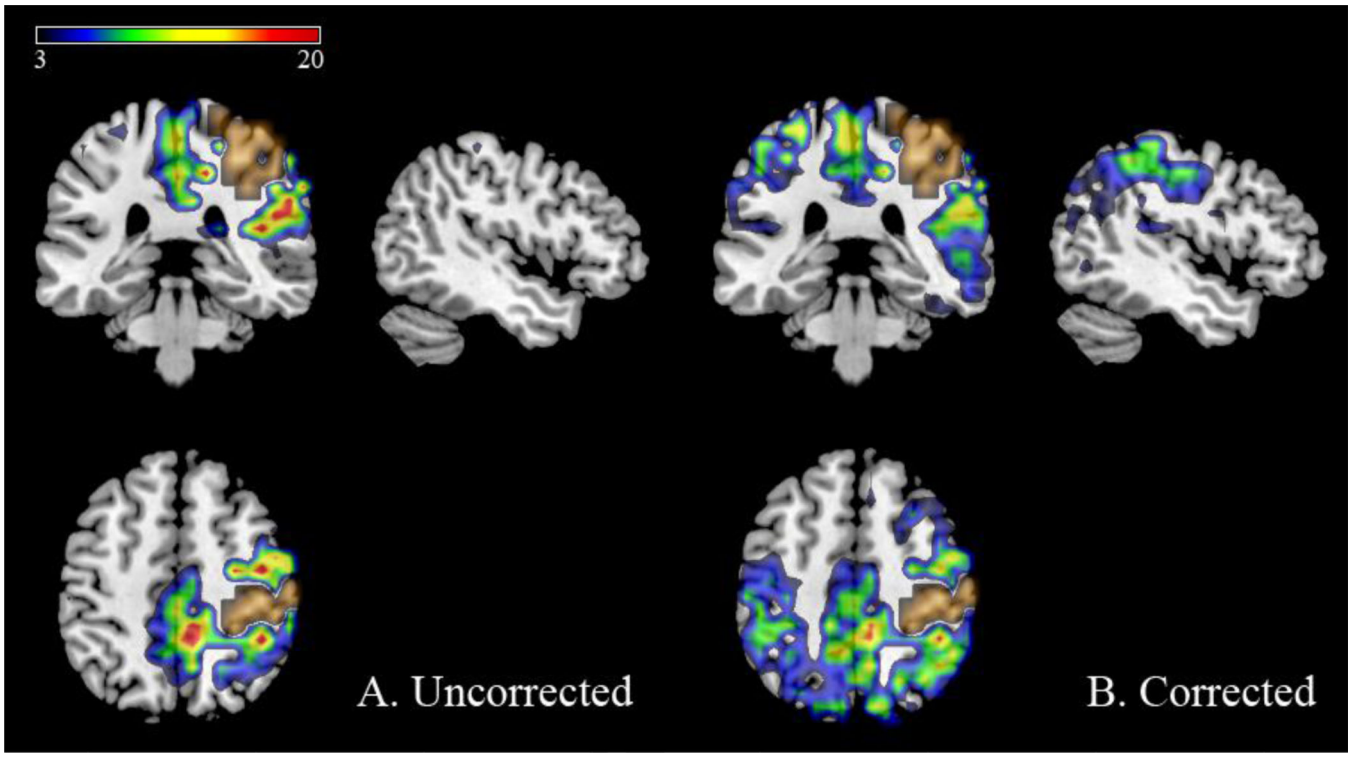

Figure 3.

Group connectivity heat map for voxels connected to the right post-central gyrus (post_r) for the non-corrected MEG data (A) and corrected data (B). The area in gold represents the seed. Uncorrected data demonstrates no significant interhemispheric connections. Following correction, robust contralateral connectivity to the primary sensor cortex is demonstrated, as well as to the bilateral supplementary motor areas near the midline.

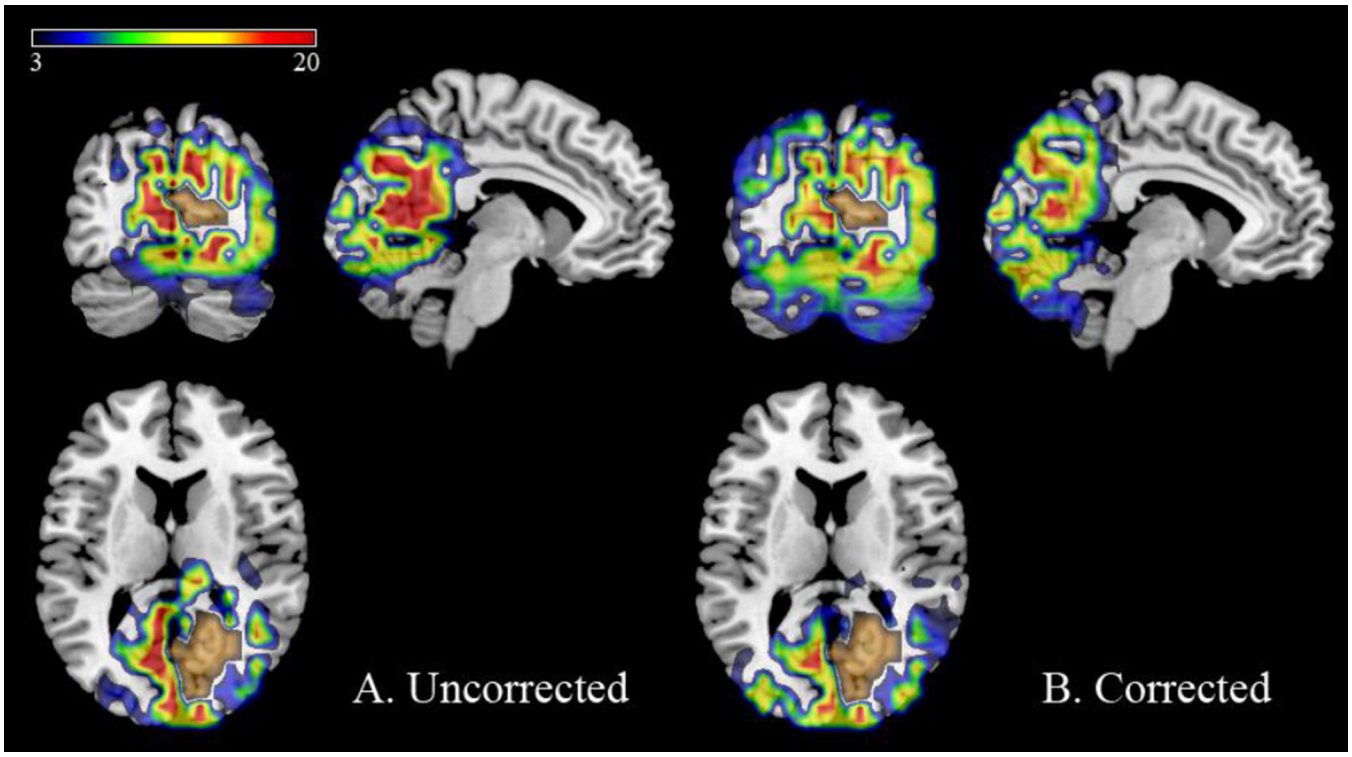

Figure 4.

Group connectivity heat map for voxels connected to the right calcarine cortex (calc_r) for the non-corrected MEG data (A) and corrected data (B). The area in gold represents the seed. Uncorrected data demonstrates no interhemispheric connections beyond a small strip of the midline immediately adjacent to primary ROI.

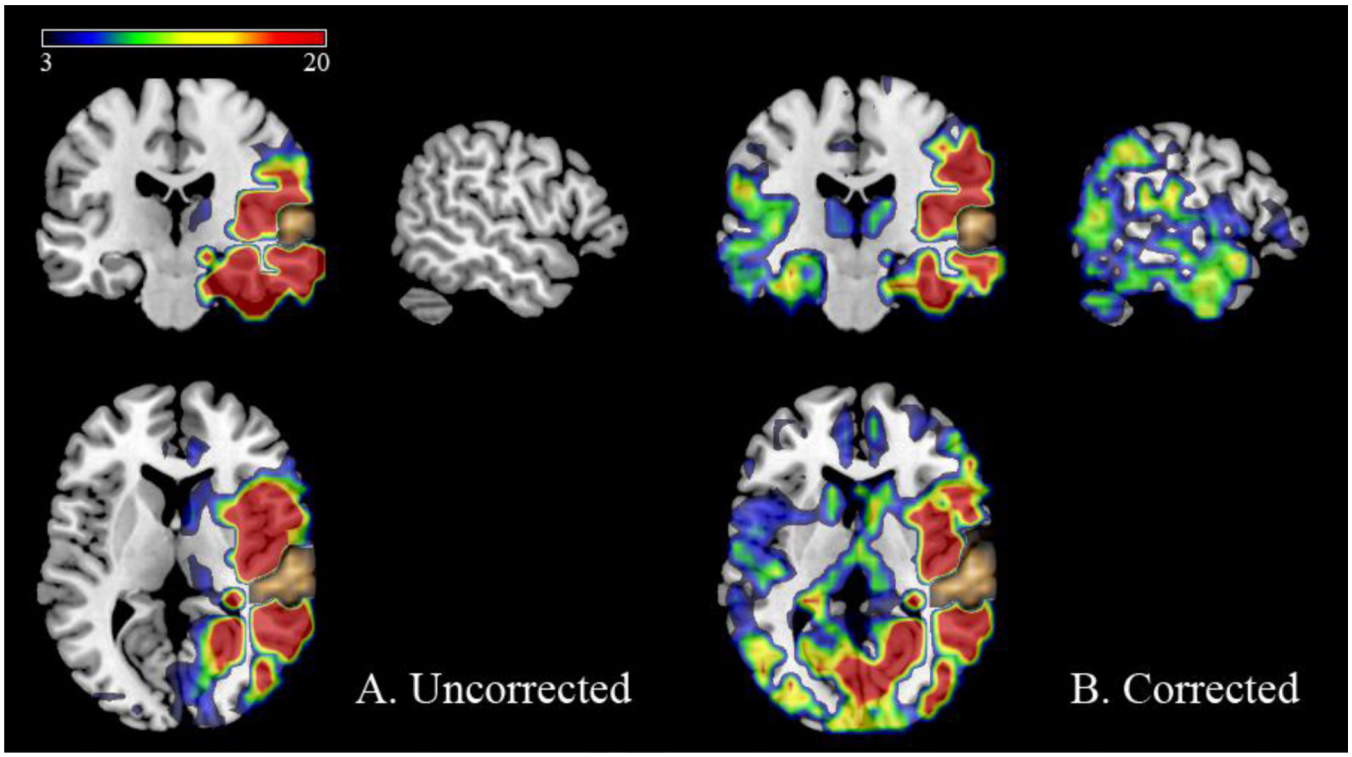

Figure 5.

Group connectivity heat map for voxels connected to the right middle temporal gyrus (temp_r) for the non-corrected MEG data (A) and corrected data (B). The area in gold represents the seed. Uncorrected data demonstrates no significant interhemispheric connections. Following leakage correction distributed areas of connectivity are demonstrated including the left temporal lobe, bilateral frontal lobes, and basal ganglia.

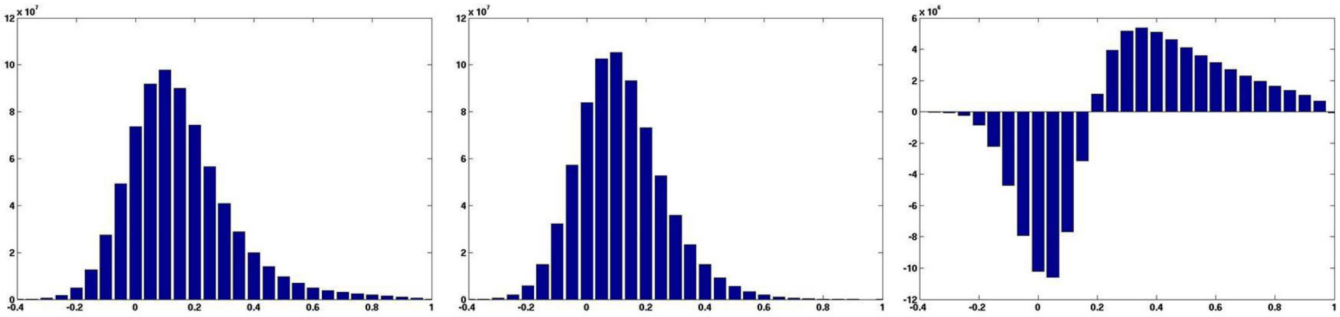

Figure 6.

Histogram plots of correlation values across subjects for the uncorrected data (left), corrected data (middle), and difference (uncorrected – corrected, right). Uncorrected data demonstrates a larger number of high-correlation edges (> 0.5) than the corrected data. Difference histogram plot demonstrates a shift towards high correlation edges for the uncorrected data, with the majority of connections in this region representing leakage.

Table 1

Degree map Laterality Indices for ROI-based connections at cost=0.05

	Pre_L		Pre_R		Post_L		Post_R		Calc_L		Calc_R		Temp_L		Temp_R	
Subject	**uc**	**c**	**uc**	**c**	**uc**	**c**	**uc**	**c**	**uc**	**c**	**uc**	**c**	**uc**	**c**	**uc**	**c**
1	0.8 2	0.7 8	−0.9 2	−0.4 2	0.9 7	0.6 9	−0.9 7	−0.5 5	0.0 4	0.1 7	−0.4 9	−0.1 6	0.9 7	0.3 3	−1.0 0	−0.6 7
2	0.9 4	0.9 0	−0.9 9	−0.8 8	0.8 8	−0.1 6	−0.9 9	−0.9 6	−0.1 4	−0.2 3	−0.5 4	−0.3 3	0.9 9	0.3 7	−0.9 9	−0.6 2
3	0.9 5	0.7 7	−0.7 7	−0.5 0	0.8 5	0.5 2	−0.8 9	−0.7 7	0.1 1	−0.3 7	−0.3 8	−0.2 7	0.9 9	0.5 7	−0.9 7	−0.6 6
4	0.9 9	1.0 0	−1.0 0	−1.0 0	1.0 0	1.0 0	−1.0 0	−1.0 0	−0.1 4	−0.2 4	−0.4 0	−0.1 4	0.7 5	−0.1 6	−0.9 2	−0.4 4
5	0.9 4	0.3 5	−0.9 5	−1.0 0	0.9 3	0.3 6	−0.9 5	−0.4 8	0.2 6	−0.3 8	−0.8 5	−0.8 2	1.0 0	0.9 5	−0.9 4	−0.6 3
6	0.9 4	0.4 5	−0.9 8	−0.4 8	0.9 8	0.7 0	−0.9 9	−0.3 7	−0.0 2	−0.1 9	−0.6 5	−0.4 3	1.0 0	0.2 7	−1.0 0	−0.5 9
7	0.9 9	0.8 5	−0.9 7	−0.9 4	0.9 8	0.8 5	−0.9 9	−0.9 3	−0.0 9	−0.4 0	−0.6 2	−0.4 9	1.0 0	0.8 4	−0.9 0	−0.6 2
8	0.9 5	0.5 4	−0.9 7	−0.3 4	0.6 6	0.0 7	−0.9 0	−0.2 2	0.3 3	0.0 8	−0.3 0	−0.0 4	0.8 7	0.1 2	−0.9 9	−0.2 0
9	0.9 7	0.7 8	−0.9 9	−0.6 0	0.9 8	−0.1 1	−0.9 5	−0.4 5	0.0 9	−0.1 0	−0.5 5	−0.1 3	1.0 0	0.0 6	−1.0 0	−0.4 1
10	0.9 5	0.6 5	−0.9 9	−0.2 1	0.9 6	0.6 5	−0.6 8	0.0 5	0.3 6	0.0 6	−0.8 2	−0.5 7	1.0 0	0.7 7	−0.9 9	−0.5 1
11	0.8 4	0.1 5	−0.7 3	−0.0 3	0.6 4	0.3 0	−0.5 6	0.0 4	0.2 2	0.0 2	−0.5 6	−0.2 6	0.9 9	0.5 8	−1.0 0	−0.4 6
12	0.9 5	0.4 6	−0.9 9	−0.2 0	0.9 9	0.4 8	−1.0 0	−0.2 7	0.2 1	−0.1 8	−0.6 5	−0.0 5	0.9 9	0.2 5	−0.9 9	−0.6 4
13	0.9 9	0.8 6	−0.9 4	−0.7 0	0.9 5	0.5 6	−0.8 8	−0.5 9	−0.2 5	−0.3 1	−0.5 6	−0.3 7	1.0 0	0.6 5	−0.9 9	−0.6 8
14	0.9 9	0.1 8	−0.9 8	0.2 7	1.0 0	0.5 7	−0.9 9	−0.2 6	0.1 6	−0.0 3	−0.4 4	−0.2 3	1.0 0	0.5 8	−0.9 9	−0.5 2
15	0.9 8	0.8 3	−0.9 9	−0.9 1	0.9 7	0.5 0	−0.9 9	−0.9 4	0.1 3	0.3 3	−0.6 6	−1.0 0	1.0 0	1.0 0	−1.0 0	−1.0 0
16	0.7 8	0.2 7	−0.4 7	−0.1 2	0.3 5	0.0 9	−0.4 8	−0.2 5	0.1 2	−0.1 0	−0.3 8	−0.3 3	1.0 0	0.9 5	−0.9 9	−0.3 8
17	0.7 8	0.6 1	−0.9 4	−0.6 3	0.7 9	0.5 7	−0.9 8	−0.7 0	0.0 4	0.1 2	−0.4 0	0.3 1	0.9 9	0.5 3	−0.9 9	−0.3 6
18	0.8 7	0.3 0	−0.9 7	−0.3 5	0.9 6	0.4 6	−0.9 8	−0.2 7	0.0 8	−0.1 8	−0.5 1	−0.2 3	1.0 0	0.6 2	−0.9 2	−0.4 1
19	0.9 9	0.1 9	−0.9 9	−0.4 8	0.8 0	0.3 2	−0.8 9	−0.2 6	0.1 6	−0.1 3	−0.4 8	−0.4 0	0.9 7	0.4 9	−1.0 0	−0.6 1
20	0.9 3	0.8 5	−0.9 5	−0.9 4	0.9 9	0.8 5	−0.9 9	−0.9 6	−0.0 3	−0.1 7	−0.6 6	−0.7 4	0.9 9	0.8 7	−1.0 0	−0.9 9
21	0.8 3	0.3 3	−0.9 6	−0.6 1	0.8 4	0.2 5	−0.9 9	−0.7 1	−0.0 5	−0.4 2	−0.5 2	−0.4 7	1.0 0	0.4 0	−0.9 9	−0.7 3
22	0.9 7	0.5 8	−0.7 5	−0.3 8	0.5 5	0.1 8	−0.7 7	−0.4 5	0.0 9	−0.0 8	−0.6 8	−0.3 6	0.9 9	0.5 8	−0.9 9	−0.7 3
Std. Error	0.0 1	0.0 6	0.0 3	0.0 7	0.0 4	0.0 6	0.0 3	0.0 7	0.0 3	0.0 4	0.0 3	0.0 6	0.0 1	0.0 7	0.0 1	0.0 4
Mean	0.9 2	0.5 8	−0.9 2	−0.5 2	0.8 6	0.4 4	−0.9 0	−0.5 1	0.0 8	−0.1 2	−0.5 5	−0.3 4	0.9 8	0.5 3	−0.9 8	−0.5 8

Pre = precentral gyrus; Post = postcentral gyrus; Calc = calcarine cortex; Temp = middle temporal gyrus
uc = uncorrected; c = corrected

LI = (left connections − right connections)/ (left + right connections)

LI = 1 or −1 means no contralateral connections